LBNL-39065
UC-410
Preprint

ERNEST ORLANDO LAWRENCE BERKELEY NATIONAL LABORATORY

Photoelectron Spectroscopy and the Dipole Approximation

O. Hemmers, P. Glans, D.L. Hansen, H. Wang,
S.B. Whitfield, D.W. Lindle, R. Wehlitz, J.C. Levin,
I.A. Sellin, and R.C.C. Perera
Accelerator and Fusion Research Division

June 1996
Submitted to
Synchrotron Radiation News

REFERENCE COPY
Does Not
Circulate
Bldg. 50 Library.
LBNL-39065
Copy 1

DISCLAIMER

This document was prepared as an account of work sponsored by the United States Government. While this document is believed to contain correct information, neither the United States Government nor any agency thereof, nor the Regents of the University of California, nor any of their employees, makes any warranty, express or implied, or assumes any legal responsibility for the accuracy, completeness, or usefulness of any information, apparatus, product, or process disclosed, or represents that its use would not infringe privately owned rights. Reference herein to any specific commercial product, process, or service by its trade name, trademark, manufacturer, or otherwise, does not necessarily constitute or imply its endorsement, recommendation, or favoring by the United States Government or any agency thereof, or the Regents of the University of California. The views and opinions of authors expressed herein do not necessarily state or reflect those of the United States Government or any agency thereof or the Regents of the University of California.

LBNL-39065
LSBL-341
UC-410

Photoelectron Spectroscopy and the Dipole Approximation

O. Hemmers, P. Glans, D.L. Hansen, H. Wang,
S.B. Whitfield, D.W. Lindle

Department of Chemistry
University of Nevada
Las Vegas, NV 89154-4003

R. Wehlitz, J.C. Levin, I.A. Sellin

Department of Physics and Astronomy
University of Tennessee
Knoxville, TN 37996-1200

R.C.C. Perera

Advanced Light Source
Accelerator and Fusion Research Division
Ernest Orlando Lawrence Berkeley National Laboratory
University of California
Berkeley, CA 94720

June 1996

This work was supported by the Director, Office of Energy Research, Office of Basic Energy Sciences, Materials Sciences Division, of the U.S. Department of Energy under Contract No. DE-AC03-76SF00098.

LSBL 34
Light Source Note:
Author(s) Initials WI 6/29/96 Date
Group Leader's initials JAP 7/3/96 Date

Photoelectron Spectroscopy and the Dipole Approximation

O. Hemmers, P. Glans, D.L. Hansen, H. Wang, S.B. Whitfield, and D.W. Lindle
Department of Chemistry, University of Nevada, Las Vegas, NV 89154-4003

R. Wehlitz, J.C. Levin, and I.A. Sellin
Department of Physics and Astronomy, University of Tennessee, Knoxville, TN 37996-1200

R.C.C. Perera
Advanced Light Source, Lawrence Berkeley National Laboratory, Berkeley, CA 94720

I. Introduction

As synchrotron-radiation users around the world know well, photoelectron spectroscopy using either ultraviolet (UV) or x-ray photons is a common technique for studying materials. Photoelectron spectroscopy is a powerful technique because it can directly probe, via the measurement of photoelectron kinetic energies, orbital and band structure in valence and core levels in a wide variety of samples: atoms, molecules, clusters, solids, surfaces, and adsorbates. The technique becomes even more powerful when it is performed in an angle-resolved mode, where photoelectrons are distinguished not only by their kinetic energy, but by their direction of emission as well. Determining the probability of electron ejection as a function of angle is an excellent probe of the different quantum-mechanical channels available to any photoemission process, because it is sensitive to phase differences among these channels. As a result, angle-resolved photoemission has been used successfully for many years to provide stringent tests of our understanding of basic physical processes underlying gas-phase and solid-state interactions with radiation, and also as a tool to probe physical and chemical structure in solids and surfaces.

One mainstay in the application of angle-resolved photoelectron spectroscopy is the well-known *dipole approximation* for photon interactions, which leads to easily characterized and quantified behavior as a function of electron ejection angle (more on this later). This electric-dipole ($E1$) approximation assumes[1] that the electromagnetic field of the photon beam, typically expressed as e^{ikr}, can be treated as a Taylor-series expansion, $1 + ikr + \ldots$, then truncated to $e^{ikr} \approx 1$. In this simplification, all higher-order terms, such as those due to electric-quadrupole ($E2$) and magnetic-dipole ($M1$) interactions, are neglected. Over the past two decades or so, the dipole approximation has facilitated a basic understanding of the photoionization process in atoms and molecules,[2,3] as well as the application of photoelectron spectroscopy to a wide variety of condensed-phase systems.

The dipole approximation was first applied to angle-resolved photoemission at a time when most experiments used relatively low photon energies, i.e., UV and far-UV radiation.[3] Since that time, however, many applications of experimental photoelectron spectroscopy have been extended to higher and higher photon energies without considering the validity of the dipole approximation as the photon energy increases. In the UV range, at least, the dipole approximation is grounded in solid physical reasoning based on two qualitative classical

arguments. First, photoelectron velocities following UV photoemission are extremely small compared to the speed of light, c, rendering relativistic effects unlikely. Second, the wavelength of ionizing UV light (e.g., He I radiation) is much larger than the size of the orbitals from which electrons are ejected, mitigating higher-order effects in the photon interaction.

With increasing photon energy, however, these simple arguments eventually must become invalid, and effects due to interactions beyond the dipole approximation must become important. It is the purpose of this report to address some of the limits of this approximation. To best determine the range of validity of the dipole approximation, photoemission measurements on a rare-gas sample, where extra-atomic effects clearly cannot play a role, were performed. The measurements show that deviations from "dipole" expectations in angle-resolved *valence* photoemission from neon are observable for photon energies down to 0.25 keV, and are quite significant at energies around 1 keV. From these results, it is clear that non-dipole angular-distribution effects may need to be considered in any application of angle-resolved photoelectron spectroscopy that uses x-ray photons of energies as low as a few hundred eV.

II. Beyond the Dipole Approximation

To see how non-electric-dipole interactions can affect photoelectron angular distributions, it is helpful to first look at the consequences of the dipole approximation for angle-resolved photoemission. The dipole approximation for photon interactions leads to the following expression for the differential photoionization cross section:[4]

$$\frac{d\sigma}{d\Omega} = \frac{\sigma}{4\pi} \left[1 + \frac{\beta}{2}(3\cos^2\Theta - 1)\right] , \tag{1}$$

which describes the angular distribution of photoelectrons from a randomly oriented sample (e.g., a gas) created by 100% linearly polarized light. Here, σ is the partial photoionization cross section for a particular subshell, and the angle Θ is measured between the polarization vector of the ionizing radiation and the momentum vector of the ejected electron (see Fig. 1). The parameter β, which can only have values in the range from -1 to 2, completely describes the angular distribution of photoelectrons within the dipole approximation. As shown in Eq. (1), the angle-resolved ejection probability for photoelectrons can be approximated as a simple combination of linear and $\cos^2\Theta$ terms, leading to angular distributions of photoelectrons that are symmetrical about the photon polarization axis (the y-axis in Fig. 1).

The first hint of low-photon-energy (i.e., ≤ 5 keV) deviations from the dipole approximation was provided by Krause[5] in measurements on rare gases using unpolarized x-rays.[6] A small deviation from the expected dipolar angular distribution at photon energies between 1 and 2 keV was observed and attributed to the influence of electric-quadrupole and magnetic-dipole interactions, which can play a role when the next term in the Taylor-series expansion for e^{ikr} is included, namely $e^{ikr} \approx 1 + ikr$. These higher-order corrections to the dipole approximation

lead to so-called *non-dipole* effects (e.g., retardation or photon momentum transfer) in the angular distributions of photoelectrons. They can be described by[7]

$$\frac{d\sigma}{d\Omega} = \frac{\sigma}{4\pi} \left[1 + \frac{\beta}{2}(3\cos^2\Theta - 1) + (\delta + \gamma\cos^2\Theta)\sin\Theta\cos\phi \right] \quad (2)$$

for 100% linearly polarized light. The angle ϕ is measured between the propagation vector of the ionizing radiation and the projection of the photoelectron's momentum vector into the x-z-plane (see Fig. 1). The non-dipole angular-distribution parameters γ and δ result from the effects of electric-quadrupole and magnetic-dipole interactions. The initial gas-phase experiments[5,8] motivated theoretical work,[9,10] and recent publications[7,11,12] include quantitative predictions for several rare-gas subshells. Recently, more extensive measurements,[13,14] focussing on noble-gas *core* levels (Ar K and Kr L) and photon energies above 2 keV, have begun to investigate non-dipole effects in photoelectron angular distributions in more detail.

Perhaps even more telling for the validity of the dipole approximation in most applications of angle-resolved photoelectron spectroscopy, the experiments described in this report concentrate on the Ne 2s and 2p *valence* subshells at lower photon energies (0.25 keV $\leq h\nu \leq$ 1.2 keV). Non-dipole effects are observed to be significant in this energy range and observable even at the lowest energy studied (0.25 keV), in conflict with a common assumption in applications of photoelectron spectroscopy; namely, that the dipole approximation is strictly valid for photon energies below 1 keV. The potential significance of these findings is nicely illustrated by comparison of our recent results[15] for the Ne β_{2p} parameter with earlier results,[8] where the influence of non-dipole effects was assumed negligible. Large differences in the measured β_{2p} parameters from the two experiments are directly attributable to "contamination" of the previous measurements[8] by non-dipole effects. Generalization of this observation to any angle-resolved-photoemission measurement suggests that relative photoemission peak intensities as a function of angle can be influenced significantly by non-dipole interactions, even at photon energies below 1 keV. Therefore, a need for caution in interpretating angle-resolved photoemission data from gases, solids, and surfaces using soft-x-ray excitation is warranted.

III. Measurements and Results

The new measurements on Ne were performed at the ALS on undulator beamline 8.0,[16] which covers the 100-1500 eV photon-energy range. Because the photon resolution needed to resolve the Ne 2s and 2p valence lines is low ($E/\Delta E \leq 200$), the monochromator slits were kept open, providing extremely high flux from the undulator source. During the measurements the ALS operated at 1.9 GeV in 2-bunch mode, yielding a photon pulse every 328 ns. This timing structure is essential for this experiment, because electron kinetic energies are determined by measuring flight times of electrons over a set distance [flight time α (kinetic energy)$^{-1/2}$]. Time-of-flight (TOF) photoelectron spectroscopy is used because it is an efficient technique in which nearly all electron kinetic energies can be sampled simultaneously.

The photoelectron-TOF system is a new apparatus that presently has 3 operational analyzers (a fourth will be available by late 1996) placed at different electron ejection angles. These analyzers are based on a new design that includes cylindrical focussing to preserve accurate timing resolution while dramatically improving the collection efficiency for highly retarded electrons. For example, in measurements with this apparatus, electrons with 1 keV initial kinetic energy were retarded to 50 eV final kinetic energy with no loss in throughput. Because electron-TOF energy resolution is directly proportional to the final kinetic energies of electrons, this new design allows efficient electron spectroscopy with energy resolution comparable to or better than most conventional electrostatic analyzers. To maintain ultimate timing resolution for this new generation of TOF analyzer, significant care was taken in the design of the microchannel-plate detectors and impedance-matched conical anodes. Likewise, the best commercially available electronic modules were obtained to allow fast simultaneous operation with up to 4 analyzers. As a result, this new system provides timing and data-collection capabilities that meet or exceed those of other electron-TOF systems in use with synchrotron radiation. Further details of the new apparatus will be presented in a forthcoming publication. Discussion of a similar apparatus is given by Becker et al.[17]

In order to measure photoelectron angular distributions, the electron-TOF analyzers can be positioned at several combinations of the angles Θ and ϕ in a vacuum chamber which can rotate about the x-ray beam. From Eq. (1), it can be shown that photoelectron peak intensities are independent of the β parameter at the so called magic angle, $\Theta_m=54.7°$. Thus, and most importantly for the present work, the chamber includes two analyzer mounting ports 54.7° out of the y-z-plane perpendicular to the x-ray-beam direction, a geometry which permits direct and sensitive measurement of non-dipole angular-distribution parameters for photoelectrons. Furthermore, the apparatus is designed so that when one TOF analyzer is positioned at $\Theta=0°$ and $\phi=90°$, a second analyzer is at $\Theta_m=54.7°$ and $\phi=90°$ (referred to as the *dipole magic-angle analyzer*) and a third analyzer is at $\Theta_m=54.7°$ and $\phi=0°$ (the *non-dipole magic-angle analyzer*). Peak intensities in the dipole magic-angle analyzer, which is in the y-z-plane (also the plane containing the ϵ-vector and perpendicular to the photon beam direction) are independent of the non-dipole parameters γ and δ [see Eq. (2)], as well as the dipole parameter β. In contrast, peak intensities in the non-dipole magic-angle analyzer are independent of the dipole parameter β, but they do depend on γ and δ.

To illustrate how non-dipole effects can perturb photoelectron angular distributions, Fig. 2 shows a few examples of how photoemission intensities change for different values of the non-dipole parameter γ. In Fig. 2, the x-y-plane is shown with the photons ($\boldsymbol{k}$) traveling in the x direction and the photon polarization vector (ϵ) along the y-axis. The red curve shows the well-known case for $\beta=2$ in the dipole approximation, where the photoelectron angular distribution is symmetrical around the y-axis. The blue curve shows the angular distribution pattern for $\gamma=1$ and $\beta=2$ and the green curve for $\gamma=2$ and $\beta=2$. (For this particular example, with $\beta=2$, the δ parameter must be zero because the differential cross section, σ, cannot be negative.[18]) Note that all three curves show the same ejection probability along the y-axis ($\phi=90°$), where the electric-quadrupole and magnetic-dipole corrections to the dipole approximation vanish. Clearly, the changes due to different γ values are quite dramatic in the forward and backward directions.

In addition, the colored areas (blue and green) show the increase of the emission probability in the direction of the non-dipole magic-angle analyzer compared to the dipole magic-angle analyzer (red area only). Not shown is the case where $\gamma < 0$, for which the same patterns appear, but directed backward, opposite the photon propagation direction.

To test the range of validity of the dipole approximation, Ne 2s and 2p valence photoemission spectra were measured over the photon-energy range from 0.25 to 1.2 keV at five different chamber rotations, yielding a total of 15 spectra, all at different Θ and/or ϕ angles, for each photon energy. Spectra were collected for about 300 s, with count rates of up to 10^5 s^{-1} in the Ne 2s photoemission peak due to the high flux from the undulator. Each set of 15 spectra provides enough information to determine simultaneously the polarization characteristics of the incident beam and the angular-distribution parameters ß, γ, and δ. It was determined that beamline 8.0 delivers nearly 100% linearly polarized light over the entire range of the experiment, provided the maximum of the undulator peak corresponds to the selected photon energy.

As an example of the observed non-dipole angular-distribution effects in Ne, Fig. 3 shows two superimposed photoemission spectra taken with $h\nu$ = 1 keV at the dipole magic angle (red) and the non-dipole magic angle (blue). The spectra are scaled to the area of the Ne KLL Auger lines. Auger lines arising from an intermediate state with an *s* hole in a closed-shell atom like Ne must have isotropic angular distributions (ß = γ = δ = 0), making them ideal for calibration.[19] Thus, angular-distribution parameters of the Ne valence peaks can be determined relative to known ß, γ, and δ parameters. The obvious intensity differences between the Ne 2s and 2p peaks in the two spectra in Fig. 3 are due entirely to non-dipole effects, because both spectra are at the magic angle where the ß parameter has no influence. Clearly, significant changes in ejection probability as a function of angle can be observed due to effects beyond the usual dipole approximation, even for valence-shell photoemission and for what is commonly considered "low" photon energies ($\leq$1 keV).

In summary, significant non-dipole effects have been observed in valence photoemission from Ne in the 0.25-1.2 keV photon-energy region. These higher-order interactions can, in principle, affect all measurements in the field of angle-resolved photoelectron spectroscopy not made in the ϕ=90° plane, even at photon energies below 1 keV. This includes not only measurements on gas-phase targets, but also surface, adsorbate, and condensed-matter targets as well. Therefore, we wish to caution users of the technique of angle-resolved photoemission that possible non-dipole effects may need to be considered when measurements are conducted at multiple ejection angles. It is conceivable that any application of photoelectron spectroscopy that relies on angle-dependent differences of photoemission intensities (e.g., much work on atoms and molecules, band-mapping in solids, photoelectron-diffraction and holography, orientation studies of adsorbates, etc.) may benefit from the consideration of non-dipole effects in their analysis. More work to determine the range of validity of the dipole approximation, in gases as well as solids, is called for.

The authors thank the staff of the ALS for their support, the IBM, LBNL, LLNL, University

of Tennessee, and Tulane University collaboration for beam time at beamline 8.0, and J.W. Cooper, C.S. Fadley, M.O. Krause, R.H. Pratt, and N.M. Kabachnik for fruitful discussions. This research is funded by the National Science Foundation, the Department of Energy, Research Corporation, and The Petroleum Research Fund. The ALS is supported by the Department of Energy under Contract No. DE-AC03-76SF00098.

References.

1. H.A. Bethe and E.E. Salpeter, *Quantum Mechanics of One- and Two-Electron Atoms* (Springer-Verlag, Berlin, 1957).
2. S.T. Manson and D. Dill, in *Electron Spectroscopy: Theory, Techniques, and Applications*, Vol. 2, edited by C.R. Brundle and A.D. Baker (Academic, New York, 1978).
3. See, for example, D.W. Turner, A.D. Baker, C. Baker, and C.R. Brundle, *Molecular Photoelectron Spectroscopy* (Wiley, New York, 1970).
4. J. Cooper and R.N. Zare, J. Chem. Phys. **48**, 942 (1968).
5. M.O. Krause, Phys. Rev. **177**, 151 (1969).
6. For unpolarized incident light, $\beta/2$ is replaced by $-\beta/4$ in Eq. (1), and Θ is measured between the propagation vectors of the photon and the photoelectron. Otherwise, the essential physics is the same.
7. J.W. Cooper, Phys. Rev. A **42**, 6942 (1990); **47**, 1841 (1993).
8. F.J. Wuilleumier and M.O. Krause, Phys. Rev. A **10**, 242 (1974).
9. M.Ya. Amusia and N.A. Cherepkov, *Case Studies in Atomic Physics*, Vol. 5 (North-Holland, Amsterdam, 1975).
10. A. Ron, R.H. Pratt, and H.K. Tseng, Chem. Phys. Lett. **47**, 377 (1977); H.K. Tseng, R.H. Pratt, S. Yu, and A. Ron, Phys. Rev. A **17**, 1061 (1978).
11. A. Bechler and R.H. Pratt, Phys. Rev. A **39**, 1774 (1989); **42**, 6400 (1990).
12. J.H. Scofield, Phys. Rev. A **40**, 3054 (1989); Phys. Scripta **41**, 59 (1990).
13. B. Krassig, M. Jung, D.S. Gemmell, E.P. Kanter, T. LeBrun, S.H. Southworth, and L. Young, Phys. Rev. Lett. **75**, 4736 (1995).
14. M. Jung, B. Krassig, D.S. Gemmell, E.P. Kanter, T. LeBrun, S.H. Southworth, and L. Young, to be published.
15. O. Hemmers, G. Fisher, P. Glans, D.L. Hansen, H. Wang, S.B. Whitfield, D.W. Lindle, R. Wehlitz, J.C. Levin, I.A. Sellin, R.C.C. Perera, E.W.B. Dias, H.S. Chakarborty, P.C. Deshmukh, and S.T. Manson (to be published).
16. R.C.C. Perera, Nucl. Instrum. Methods **A319**, 277 (1992).
17. U. Becker, D. Szostak, H.G. Kerkhoff, M. Kupsch, B. Langer, R. Wehlitz, A. Yagishita, and T. Hayaishi, Phys. Rev. A **39**, 3902 (1989).
18. In general, the allowed values of γ and δ depend on the value of β. By recognizing that the differential cross section, $d\sigma/d\Omega$, in Eq. (2) cannot be negative at any ejection angle, the following inequalities for δ and γ can be approximated: $\frac{1}{2}\beta-1 \leq \delta \leq 1-\frac{1}{2}\beta$, and $-3[\delta+(3/2)^{1/2}] \leq \gamma \leq 3[(3/2)^{1/2}-\delta]$. For the specific example cited in the text, with $\beta=2$, we find $\delta=0$ and $-3(3/2)^{1/2} \leq \gamma \leq 3(3/2)^{1/2}$.
19. S. Flugge, W. Mehlhorn, and V. Schmidt, Phys. Rev. Lett. **29**, 7 (1972).

Figure Captions.

Fig. 1. Geometry applicable to photoelectron angular-distribution measurements using polarized light. Θ is the polar angle between the photon polarization vector ϵ and the momentum vector $\boldsymbol{p}$ of the photoelectron. ϕ is the azimuthal angle defined by the photon propagation vector $\boldsymbol{k}$ and the projection of $\boldsymbol{p}$ into the x-z-plane.

Fig. 2. Photoelectron ejection probability patterns for three sets of angular-distribution parameters. For all three cases, $\beta=2$ and $\delta=0$. The γ parameter has the values zero (red curve), 1 (blue curve), and 2 (green curve). One electron-TOF analyzer is placed at the non-dipole magic angle ($\Theta_m=54.7°$, indicated by the arrow) in the x-y-plane where the photoelectron ejection probability depends on γ and δ but not on β. Colored areas represent changes in ejection probability in the direction of this analyzer for different values of γ.

Fig. 3. Photoelectron spectra of Ne measured at a photon energy of 1 keV. The red spectrum was taken with the dipole magic-angle analyzer and the blue spectrum with the non-dipole magic-angle analyzer. At this photon energy, we find that $\gamma \approx 1$ and $\delta \approx 0$, in accord with the blue curve in Fig. 2.

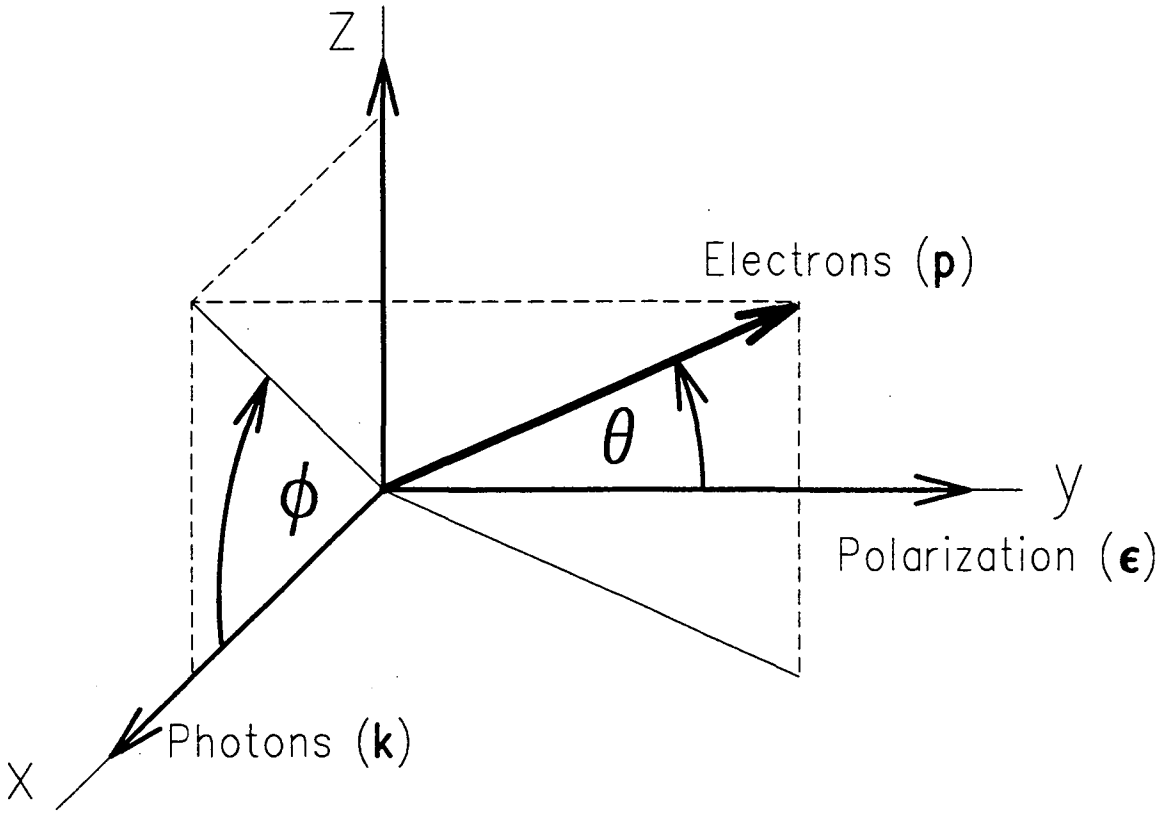
Z
Electrons (**p**)
θ
ϕ
y
Polarization (**ϵ**)
Photons (**k**)
X

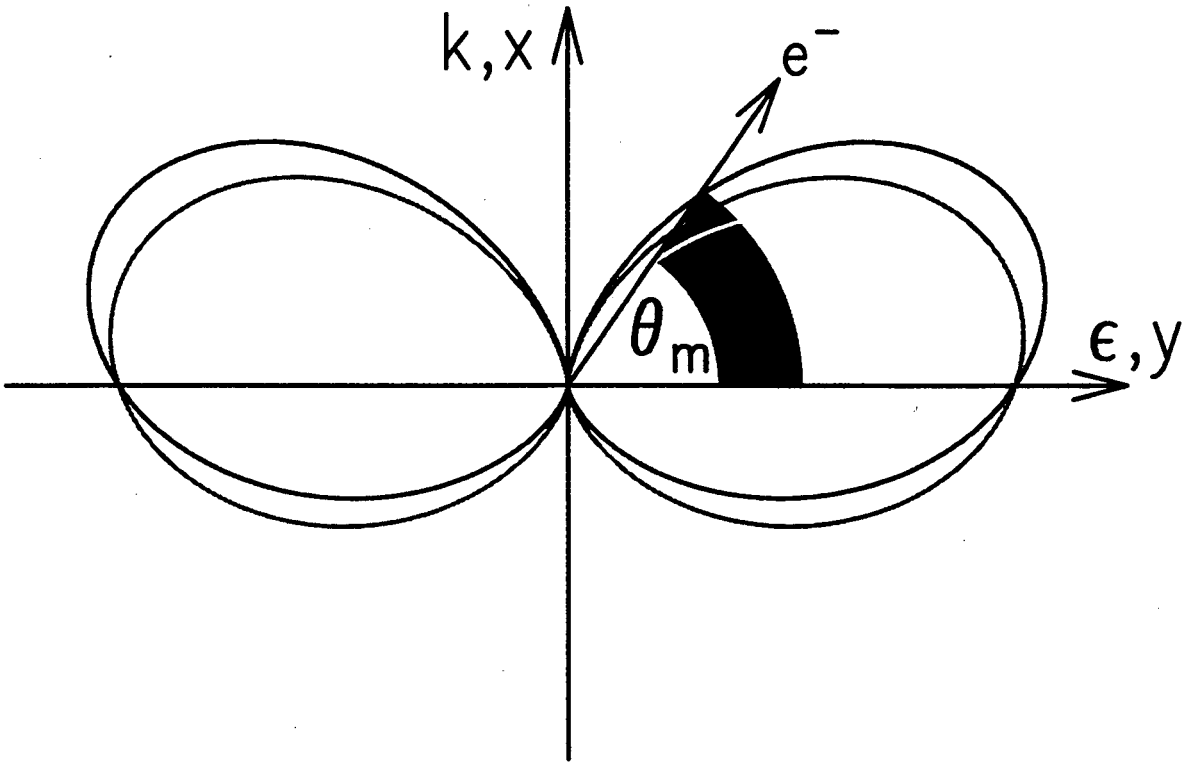
k,x
e⁻
θm
ϵ,y

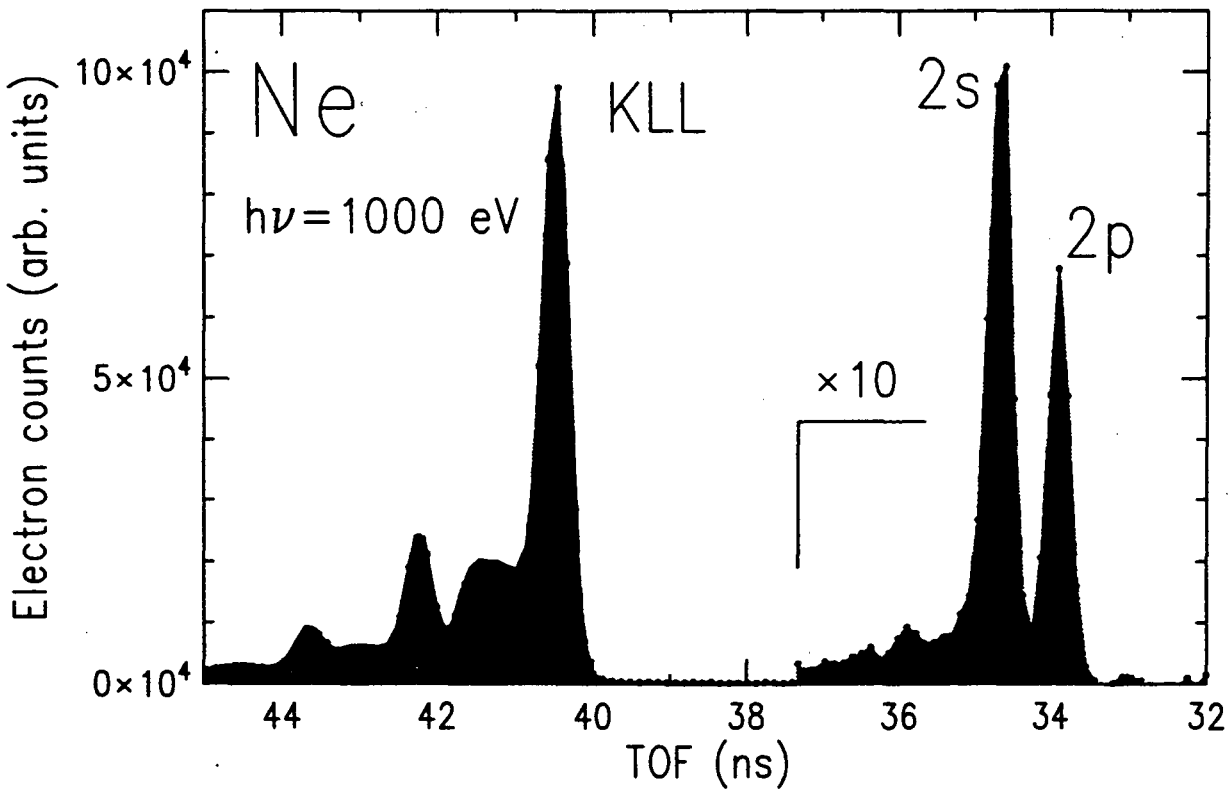
Ne
KLL
2s
2p
hν=1000 eV
×10
10×10⁴
5×10⁴
0×10⁴
Electron counts (arb. units)
44
42
40
38
36
34
32
TOF (ns)

Ernest Orlando Lawrence Berkeley National Laboratory
One Cyclotron Road | Berkeley, California 94720

Prepared for the U.S. Department of Energy under Contract No. DE-AC03-76SF00098